Reactive and Functional Polymers 180 (2022) 105387

Contents lists available at ScienceDirect

Reactive and Functional Polymers

journal homepage: www.elsevier.com/locate/react

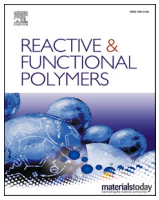

Synergistic effect of type and concentration of surfactant and diluting solvent on the morphology of emulsion templated matrices developed as tissue engineering scaffolds

Betül Aldemir Dikici [a,b,c,*], Serkan Dikici [a,b], Frederik Claeyssens [b,c,*]

[a] Department of Bioengineering, Izmir Institute of Technology, Urla, Izmir 35430, Turkey
[b] Kroto Research Institute, Department of Materials Science and Engineering, University of Sheffield, Sheffield, United Kingdom
[c] Department of Materials Science and Engineering, INSIGNEO Institute for In Silico Medicine, The University of Sheffield, Sheffield, United Kingdom

ARTICLE INFO

Keywords:
Biomaterials
Tissue engineering
Emulsion templating
PolyHIPE
Pore size
Porosity

ABSTRACT

Emulsion templating is an advantageous route for the fabrication of tissue engineering scaffolds. Emulsions are mostly stabilised using surfactants, and the performances of the surfactants depend on various parameters such as emulsification temperature and the presence of the electrolytes. In this study, we suggest that diluting solvent type also has a dramatic impact on the efficiency of the surfactant and morphology of the polymerised emulsions. For this, morphologies of polycaprolactone methacrylate-based polymerised emulsions, which are designed for tissue engineering applications and *in vitro* biocompatibilities, were shown by our group, prepared using four different surfactants, and three different solvents were investigated. Results showed that the diluting solvent used in the emulsion composition has a strong impact on the performance of the surfactant and consequently on the morphology of polymerised emulsions. Increasing surfactant concentration and diluting solvent volume have an opposite impact on the characteristics of emulsions. Scaffolds with average pore sizes changing from 10 to 78 μm could be fabricated. Establishing these relations enables us to have control over the overall morphology of polymerised emulsions and precisely engineer them for specific tissue engineering applications by tuning solvent and surfactant type and concentration.

1. Introduction

Over the years, emulsion templated matrices have been used in various areas such as fabrication of catalyst supports, membranes, separation columns, substrates for electrodes, solid-phase synthesis, absorption, adsorption, drug delivery, and encapsulation [1–7].

Recently, emulsion templating has also gained particular attention as a scaffold fabrication technique in the field of tissue engineering [8–21]. Scaffolds are porous matrices that serve as a temporary 3-dimensional substrate and provide mechanical support to the defect region over the tissue regeneration process. The porosity of a tissue engineering scaffold is crucial for the nutrient exchange, cell infiltration, and effective delivery of biofactors. In addition, the tunability of the scaffolds enables the fabrication of matrices for specific hard and soft tissue applications. Emulsion templating is a favourable scaffold fabrication route due to the following advantages: providing (i) high porosity (up to 99% [22]), (ii) high interconnectivity, (iii) high tunability [8,23–25], and (iv) being appropriate to be combined with other fabrication techniques (such as 3D printing [11,15,26] and electrospinning [27]) for the fabrication of more complex structures.

Emulsion templating is based on creating a stable emulsion by mixing two immiscible liquids and then polymerising the continuous phase (Fig. 1A–H) [15]. Emulsion droplets act as a pore template during polymerisation, and they are removed afterwards. When the internal phase volume (total droplet volume) of the emulsion is between 30 and 74%, the emulsion is defined as Medium Internal Phase Emulsion (MIPE), and when it is greater than 74%, it is defined as a High Internal Phase Emulsion (HIPE) [28]. However, the presence of two immiscible liquids in a composition of emulsions results in a high level of surface tension at their interfaces, and this situation may cause destabilisation of the emulsions due to coalescence, Oswald ripening, flocculation, creaming, or phase separation [29]. In most cases, surfactants are used

* Corresponding authors at: Department of Bioengineering, Izmir Institute of Technology, Urla, Izmir, 35430, Turkey and Kroto Research Institute, Department of Materials Science and Engineering, University of Sheffield, Sheffield, United Kingdom.
E-mail addresses: betulaldemir@iyte.edu.tr (B. Aldemir Dikici), f.claeyssens@sheffield.ac.uk (F. Claeyssens).

https://doi.org/10.1016/j.reactfunctpolym.2022.105387
Received 4 May 2022; Received in revised form 1 August 2022; Accepted 24 August 2022
Available online 31 August 2022

to stabilise these emulsion systems. These amphiphilic compounds prevent destabilisation by creating a barrier between the oil and water phases and reducing the interfacial tension. To date, a wide range of surfactants has been proposed for their use in the stabilisation of emulsions. The surfactant choice [30–32] and concentration [9] play an important role in emulsion stability and a deterministic role in the morphologies of polymerised MIPEs (PolyMIPEs) and polymerised HIPEs (PolyHIPEs). Surfactants are categorised based on their hydrophile-lipophile balance (HLB), a scale described by Griffin [33,34], and a quantitative representation of the Bancroft rule [35]. The HLB value is in direct correlation with the hydrophilicity of the surfactant [36]. While surfactants with low HLB values are good for water-in-oil (w/o) emulsions, surfactants with high HLB values are more suitable for oil-in-water (o/w) emulsions [36]. Although this value gives an insight into the initial surfactant choice, as the performances of the surfactants are reported to depend on various parameters such as emulsification temperature, the solubility of the surfactant, and the absence/presence of the electrolyte [28,36], the best working surfactant is needed to be determined empirically. Indeed, many researchers reported that HLB value on its own is not enough to select a suitable surfactant for emulsion systems [30,37].

Polycaprolactone (PCL) is one of the most widely used synthetic polymers in biomedical applications due to its biocompatibility, tuneability, being suitable to be used in both hard and soft tissue engineering applications, having less acidic breakdown products compared to its counterparts, and the presence of the FDA approved PCL-based products in the clinics [9,38]. Over the years, fabrication of the PCL-based PolyHIPE has been reported to be problematic due to the high viscosity of the polymer, which limits the emulsification of the two phases [[37] 39–41]. When the polymers that will be used in the emulsification process are solid-state or in a liquid phase with high viscosity, diluting/porogenic solvents are used to reduce the viscosity of the polymer phase [17,42].

Recently, we have reported the manufacturing route of PolyHIPEs made of photocurable PCL tetra-methacrylate (4PCLMA) by optimising the diluting solvent composition [9]. In the follow-up studies, the *in vitro* biocompatibility of the material was shown using human dermal fibroblasts [9], mouse post-osteoblasts/pre-osteocytes [14,15], human endothelial cells [16], and human mesenchymal progenitor cells [15]. *In vivo* biocompatibility and suitability of the morphology to support blood vessel ingrowth were shown using chick chorioallantoic membrane assay [14,15,43]. However, in all those studies, very similar HIPE compositions were used, and the tunability of the material remained limited.

In the main study, Hypermer B246 was used as a sole surfactant to stabilise the HIPEs [9]. When the emulsion composition was prepared without using any diluting solvent, PolyHIPE failed to form due to its high viscosity, as shown in Fig. 2A. The emulsion compositions prepared using chloroform as a diluting solvent successfully formed typical open-porous (Fig. 2B) PolyHIPE morphology. However, other groups prepared using toluene as a diluting solvent failed the form a porous structure (Fig. 2C). Then, the same compositions were prepared without any surfactant, and the polymerised structures were investigated. Interestingly, both compositions (diluted with chloroform or toluene) showed porous morphology in the absence of the surfactant *(emulsions were not stable as no surfactant was used, so they were prepared and polymerised immediately to capture the morphology,*Fig. 2C *and*Fig. 2D*)* [9].

This observation showed us that in addition to other well know parameters such as emulsification temperature, the solubility of the surfactant, and the absence/presence of the electrolytes, the presence and nature of the solvent system used in the emulsion composition may also affect the performance of the surfactant. As this was not the main focus

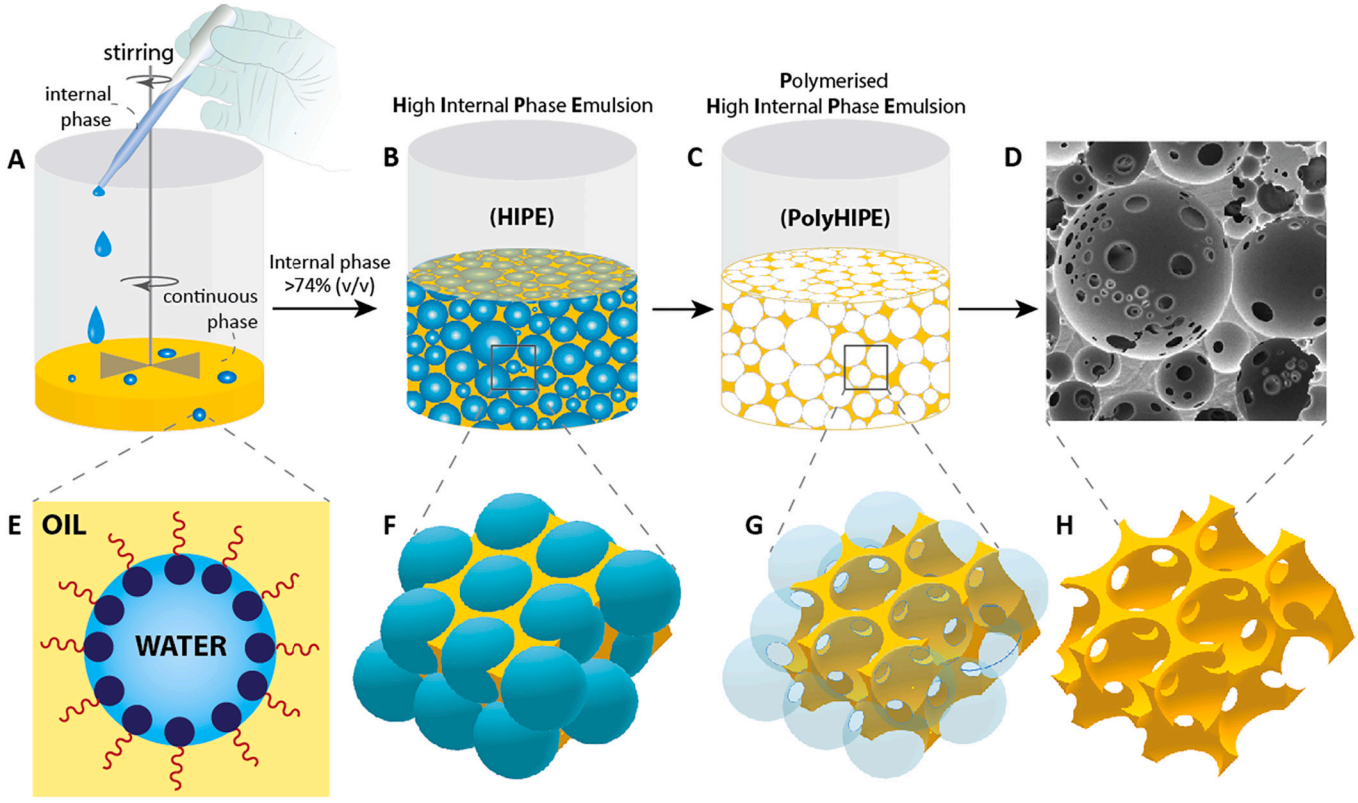

Fig. 1. Polymerised High Internal Phase Emulsion (PolyHIPE) synthesis steps. (A, B) The gradual addition of the internal phase into the continuous phase while the system is mixed, (C) polymerisation of the high internal phase emulsion (HIPE), and (D) scanning electron microscope image of the PolyHIPE. (E–H) A closer look into the system. (E) Position of surfactant molecules at the water-oil interface, (F–H) position and removal of the water droplets, and the formation of the pores and interconnects.

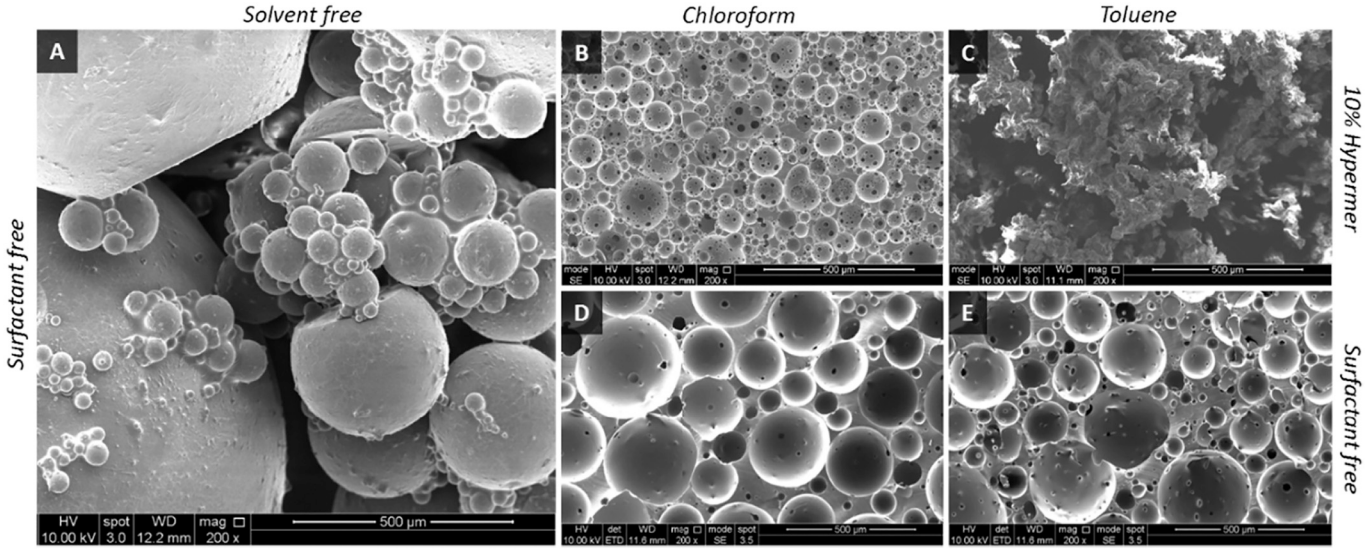

Fig. 2. Scanning electron microscope (SEM) image of (A) the surfactant-free and solvent-free composition. SEM images of 4PCLMA PolyHIPEs, prepared in the presence of the surfactant (Hypermer B246, 10% (w/w) of the polymer), using (B) chloroform as a diluting solvent and (C) toluene as a diluting solvent. SEM image of 4PCLMA PolyHIPE prepared in the absence of any surfactant by using (D) chloroform as a diluting solvent and (E) toluene as a diluting solvent. The image was adapted from [9] under The Creative Commons License.

of that study, these observations were only noted and reported as to be merited further investigation in the follow-up studies to clarify the importance of solvent-surfactant interactions in these systems.

The impact of nature and amount of diluting solvents on PolyHIPE morphology has been questioned and investigated by many other researchers. Cameron and Barbetta et al. reported the morphological differences in poly(propylene fumarate) (PPF)-based PolyHIPEs when different diluting solvents are used. They attributed this difference to the solubility of the polymers in different solvents, which are estimated using Hildebrand solubility parameters [44]. Christenson et al. investigated the impact of solvent volume on the PolyHIPE morphology [17]. Monglia et al. investigated the performance of five different surfactants in a study on the development of injectable PolyHIPEs based on propylene fumarate dimethacrylate (PFDMA) [30]. As the material is developed for injectable tissue engineering applications, the composition does not include any solvent. They concluded that the position of the hydrogen bond donor sites (either in the polar head or the hydrophobic tail) of the surfactants impacts their performances. However, none of these studies neither studied nor emphasised that there is another important fact; the solvent type has an impact on the performance of the surfactant and the choice of solvent surfactant type and the ratio has an impact on both emulsion stability and PolyHIPE morphology.

Accordingly, in this study, we hypothesised that diluting solvent type has an impact on the efficiency of the surfactant and morphology of the polymerised emulsions. We aimed to establish this relationship to enable tunability of the material using solvent and surfactant type and concentration. For this, twelve compositions of 4PCLMA-based emulsions were prepared using four different types of surfactants and three types of diluting solvents, and the morphologies of the resultant PolyMIPEs were investigated to establish a relation. Furthermore, changing solvent and surfactant concentrations and their synergistic effect on the PolyMIPE morphology were also studied. Finally, the maximum internal phase volumes, an indication of increased scaffold porosity, that can be incorporated into the 4PCLMA-based emulsion composition were investigated. Overall, independent from the monomer type, our study suggests that surfactant solvent interaction is also an important factor that should be taken into consideration in the process of developing an emulsion system both to improve the stability of emulsion systems and to control the morphology of PolyMIPEs/PolyHIPEs for specific tissue engineering applications.

2. Experimental

2.1. Materials

Pentaerythritol (98%), ε-caprolactone, tin (II) 2-ethylhexanoate, triethylamine (TEA), methacrylic anhydride (MAAn), photoinitiator (2,4,6-Trimethylbenzoyl Phosphine Oxide/2-Hydroxy-2-Methylpropio phenone blend), hydrochloric acid (HCl), Span 80, and Pluronic L121 were purchased from Sigma Aldrich (Poole, UK). Chloroform, toluene, dichloromethane (DCM), and 1,2-dichloroethane (DCE) were purchased from Fisher Scientific (Pittsburgh, PA, USA). Polyglycerol polyricinoleate 4125 (PGPR) was kindly donated by Paalsgard (Juelsminde, Denmark). The surfactant Hypermer B246 was received as a sample from Croda (Goole, UK).

2.2. Methods

2.2.1. Polymer synthesis

The detailed synthesis of the polymer, 4PCLMA, has been described elsewhere [9,14,15,45]. Briefly, under nitrogen flow, pentaerythritol (0.088 mol) and ε-caprolactone (0.353 mol) were added into a three-neck round-bottomed flask, and the system was heated to 160 °C using an oil bath while being mixed at 200 rpm. When the pentaerythritol was completely dissolved, the catalyst, tin(II) 2-ethyl hexanoate, was added, and the system was left overnight to form 4PCL before being removed from the oil bath and left to cool down in the ambient atmosphere.

4PCL was dissolved in 300 mL of DCM, and then TEA (0.52 mol) was added. Reagents were stirred, and a further 200 mL of DCM was added to ensure everything was dissolved. The flask was placed in an ice bath. MAAn (0.52 mol) was dissolved in 100 mL DCM and transferred into a dropping funnel (~1 drop per second). When the MAAn was completely dispensed, the ice bath was removed, and the system was maintained at room temperature (RT) for 68 h while being mixed. It was then washed with HCl solution and then with deionised water (dH_2O) to remove TEA, MAA, and salts formed. Almost all solvent was evaporated using a rotary evaporator. Three methanol washes were applied, and any remaining solvent was removed using a rotary evaporator. 4PCLMA was stored in

the freezer (−20 °C) for further use.

2.2.2. Nuclear magnetic resonance (NMR) spectroscopy

To confirm the structure of 4PCLMA proton (^{1}H), nuclear magnetic resonance (NMR) spectroscopy analysis was performed on an AVANCE III spectrometer at 400 MHz. The spectra were recorded using an 8.2 kHz acquisition window, with 64 k data points in 16 transients with a 60 s recycle delay (to ensure full relaxation). Deuterated chloroform was used as a diluent ($CDCl_3$). Spectra were analysed using MestReNova software. Chemical shifts were referenced relative to $CDCl_3$ at 7.26 ppm.

2.2.3. Investigating the solvent-surfactant interaction

Throughout this study, the only polymer used was 4PCLMA, and it has been entitled as PCL in the rest of the text except Section 3.1 unless otherwise stated. In this section, twelve compositions of 4PCLMA-based emulsions were prepared using four types of surfactant (Hypermer, Span 80, Pluronic L121 or PGPR) and three types of diluting solvent (chloroform, toluene or DCE). PCL (0.2 g) and 10% (*w*/w) surfactant were added into a glass vial (Ø = 25 mm). Only Hypermer B246 groups were heated to 40 °C to dissolve surfactant as it is in a wax form at RT (other surfactants are in liquid form at RT) and left for cooling. 0.2 mL solvent and photoinitiator (20% of the polymer, (w/w)) were added to the PCL-surfactant mixture and mixed at 375 rpm using a magnetic stirrer (8 × 20 mm) for 1 min at RT. Once the homogeneous mixture was created, 1 mL water was added dropwise for PCL MIPEs, and the emulsion was mixed for a further 1 min at 375 rpm. 4PCLMA MIPE was poured into circular silicon moulds and immediately (within 10 s) cured once prepared to capture the microstructure before any possible breakdown. They were cured for 5 min on both sides using the OmniCure Series 1000 curing system (100 W, Lumen Dynamics, Canada). The resulting parts were recovered from the silicon mould and soaked in methanol for removal of non-cured material, surfactant, and photoinitiator for 24 h. Following this, the samples were gradually transferred to increasing concentrations of water (50%, 100%) and then left in 100% water for a day. The samples were taken out from the water and left in a − 80 °C freezer for an hour, then transferred into the vacuum oven and left for a day to preserve the porous structure.

2.2.4. Investigating the effect of diluting solvent volume and surfactant concentration on the morphology

PGPR and DCE were selected as a surfactant and a diluting solvent, respectively, for the rest of the study. Nine groups of PolyMIPEs were prepared in this section. Three different PGPR concentration: 5%, 10%, and, 15% (of the polymer, *w*/w) and three different diluting solvent volume: 0.2 mL, 0.4 mL, and 0.6 mL (per batch) were used. As explained in Section 2.2.3, PCL (0.2 g), a photoinitiator, changing amounts of surfactant and diluting solvent were added into a glass vial mixed at 375 rpm for 1 min at RT. Once the homogeneous mixture was created, 1 mL water was added dropwise, and it was mixed for a further 1 min at 375 rpm. MIPEs were polymerised, washed and dried by following the same protocol explained in Section 2.2.3.

2.2.5. Investigating the effect of diluting solvent volume and surfactant concentration on the maximum internal phase volume that can be incorporated into 4PCLMA-based emulsion composition

Similar to Section 2.2.4. nine groups of PolyHIPEs were prepared in this section. Three different PGPR concentration: 5%, 10%, and, 15% (of the polymer, *w*/w) and three different diluting solvent volume: 0.2 mL, 0.4 mL, and 0.6 mL (per batch) were used. The oil phase was prepared in the same way, and once the homogeneous mixture was created, water was added dropwise. The water was added until the emulsion did not accept any more water (when the emulsion was saturated with the internal phase and water droplets started to accumulate on the top of the emulsion). The amounts of water that could be incorporated into HIPE compositions were recorded. HIPEs were then polymerised, washed, and dried following the same protocol explained in Section 2.2.3.

2.2.6. Nomenclature

For Section 2.2.3, where solvent-surfactant interaction was investigated, the PolyMIPE samples are referred to using a code of the form A_B where A is the type of the surfactant (H for Hypermer B246, S for Span 80, PL for Pluronic L121 and P for PGPR), B is the type of solvent used (T for toluene, C for chloroform, and D for DCE). As the amounts of surfactant and solvent used in this section are constant in all groups (reported in Section 2.2.3), their amounts are not indicated in the code. For example, the PolyMIPE sample that is prepared using Hypermer B246 as a surfactant and toluene as a solvent is abbreviated as H_T.

For Section 2.2.4, where the effect of diluting solvent volume and surfactant concentration on the morphology of PolyMIPEs were investigated, the PolyMIPE samples are referred to using a code of the form Ac_Bd where A is the type of the surfactant, c is the concentration of the surfactant, B is the type of the diluting solvent and d is the volume of the diluting solvent. For example, the PolyMIPE sample that is prepared using 5% PGPR as a surfactant and 0.2 mL DCE as a solvent is abbreviated as P5_D0.2.

For Section 2.2.5, where we investigated the effect of diluting solvent volume and surfactant concentration on the maximum internal phase volume that can be incorporated, the PolyHIPE samples are referred to using a similar code with Section 2.2.4. They are coded in the form of Ac_Bd; however, a prime sign was also included to differ the samples of this group from samples from Section 2.2.4. (Ac_Bd').

Throughout the text, "emulsion", "MIPE", and "HIPE" terms are used to refer to the compositions before the polymerisation, and "PolyMIPE" and "PolyHIPE" terms are used to refer to the structure after polymerisation.

2.2.7. Morphological investigation using scanning electron microscopy

Scanning electron microscopy (SEM) was used to investigate the microarchitecture of the scaffolds. Samples were cut from the section using a scalpel and placed on SEM pins with carbon pads. They were gold sputter-coated in 15 kV for 2.5 min to increase conductivity (5 nm). A FEI Inspect F SEM (Philips/FEI XL-20 SEM, Cambridge, UK) was used with 10 kV power [9,46,47]. 90 pores and 90 windows were randomly selected from three different SEM images, and measurements were taken. A statistical correction factor ($2/\sqrt{3}$) was applied to pore measurements to adjust the underestimation of diameter because of uneven sectioning [48]. Pore (D) and window size (d) distribution histograms were created, and average pore and window sizes were reported. The degree of interconnectivity (DI) was calculated by dividing the average window size by the average pore size (d/D) [9,49], and the degree of openness (DOO) was calculated by dividing open surface area by total surface area for randomly selected 10 pores. For this, as suggested by Pulko et al. and Owen et al., the open surface area was calculated from the surface area of the windows (as they are the open portion of the spheroid-like pores), and this value was divided by the surface area of the pore [10,50].

2.2.8. Density measurements and porosity

The densities of PolyMIPEs/PolyHIPEs were calculated using the gravimetric method using the bulk and true density of the material [51]. The porosities were calculated using Eq. 1 [52,53].

$$\%Porosity = \left(1 - \frac{\rho_{PolyMIPE/PolyHIPE}}{\rho_{wall}}\right) \times 100 \quad (1)$$

where $\rho_{PolyMIPE/PolyHIPE}$ is the PolyMIPE/PolyHIPE density and ρ_{wall} is the density of the wall. For the density of the wall, the measured density of the bulk polymer was used. Three samples were used for each group for density and porosity calculations.

3. Results and discussion

3.1. 4PCLMA synthesis

The chemical structure and ^{1}H NMR spectra of 4PCLMA are given in Fig. 3. The peaks of the methacrylate group, which show the degree of methacrylation, are labelled with A, B and C. As all methylene groups adjacent to hydroxyl end groups of PCL were converted into methacrylate, there is no corresponding peak at 3.6 ppm. So, 4PCLMA used in this study is almost 100% methacrylated.

4PCLMA-based PolyHIPE was introduced into the literature by our group [9], and all research on the development and the discovery of the potential of the material is still limited by our studies. The material was designed and tested for different soft and hard tissue engineering applications [14–16].

In all those studies, the composition of the HIPE used was composed of the following elements; 4PCLMA (with changing degrees of methacrylation), Hypermer B246 as a surfactant (10% of the polymer, *w*/w), 10–20% photoinitiator (2,4,6-trimethyl benzoyl phosphine oxide/2-hydroxy-2-methylpropiophenone blend) and solvent blend (made of changing ratios of chloroform and toluene). The only attempt to change and control the morphology of 4PCLMA PolyHIPEs was to change the ratio of chloroform and toluene in the solvent blend. It was an effective method to a large extent, but it has limited potential. For example, the maximum amount of water that could be incorporated into that composition was limited. 4PCLMA PolyHIPEs prepared using a different surfactant, and solvent types; the effect of solvent volume, surfactant concentration on the PolyHIPE morphology, and solvent surfactant interaction were still needed to be discovered to be able to have better control on the final design for specific applications. For this need, in this study, we decided to explore the effect of solvent and surfactant-related parameters on the morphologies of 4PCLMA PolyMIPs and PolyHIPEs more deeply.

3.2. The diluting solvent type has a strong impact on the efficiency of different surfactants and the morphology of PolyMIPEs

To investigate the effect of diluting solvent type on the efficiencies of surfactants and morphology of PolyMIPEs, the weight of the polymer (0.2 g), the weight of the surfactant (0.02 g), and the volume of the solvent were (0.2 mL) kept constant. As the solvent is used as a diluting agent, its volume was kept constant rather than its weight, and the polymer/diluting solvent ratio (*w*/*v*) is 1 for this section. The molecular weights of the surfactants that were tested are significantly different (ranging from 428 g/mol to 5000 g/mol) (Fig. 4). Thus, during the experimental design stages, we questioned if we should keep the molarity of the surfactant constant rather than its total weight. However, as keeping the surfactant weight concentration was the accepted method used in the literature to compare different surfactants, the same protocol was followed [54–57]. However, the influence of the molecular weight of the surfactants is definitely meriting further investigation.

The first tested surfactant was Hypermer B246 (Mw: 5000 g/mol) which is an ABA block copolymer (polyhydroxystearic acid-polyethylene glycol-polyhydroxystearic acid) based non-ionic surfactant with an HLB value of 4.6 (Fig. 4). It is in wax form at RT and insoluble in water. When Hypermer was used as a surfactant, the composition diluted with chloroform resulted in typical open cellular PolyMIPE morphology (Fig. 5, H_C). However, toluene diluted composition did not result in porous morphology (Fig. 5, H_T). These are similar results that were obtained in our previous study [9]. DCE has been tested in 4PCLMA MIPE composition as a diluting solvent first time for this composition in this study. It also exhibited open porous morphology (Fig. 5, H_D). Similar to our finding, the successful use of DCE as a diluting solvent in the composition of PCL-triacrylate (PCL-TA) based thiol-ene PolyHIPEs stabilised by Hypermer B246 has been reported previously. The polymer/diluting solvent ratio (*w*/*v*) was 0.66. It has been reported that PolyHIPEs showed open cellular porosity with an average pore size of 60 μm. 90% internal phase volume was incorporated into these structures, and this value was reported as nominal porosity [18]. There are also other studies that report the development of acrylate-based HIPE systems stabilised using Hypermer B246 as a surfactant and DCE [58,59] or chloroform [60] as a diluting solvent.

In our previous study, we reported that toluene alone as a diluting solvent was not successful for the fabrication of porous 4CPLMA PolyHIPE in changing solvent volumes. Chloroform diluted PolyHIPEs showed porous morphology in a determined solvent volume, but as chloroform volume was increased, HIPEs started to destabilise, and when the volume was reduced, the HIPE could not be formed due to high

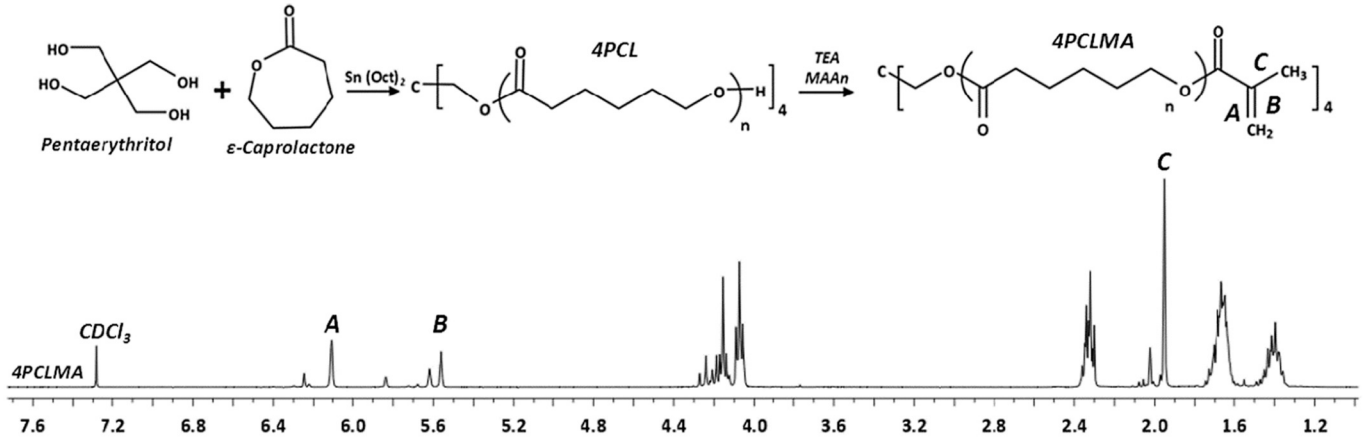

Fig. 3. ^{1}H NMR spectrum of 4PCLMA used in this study and relative assignment indicated as letters in the spectrum and chemical structures.

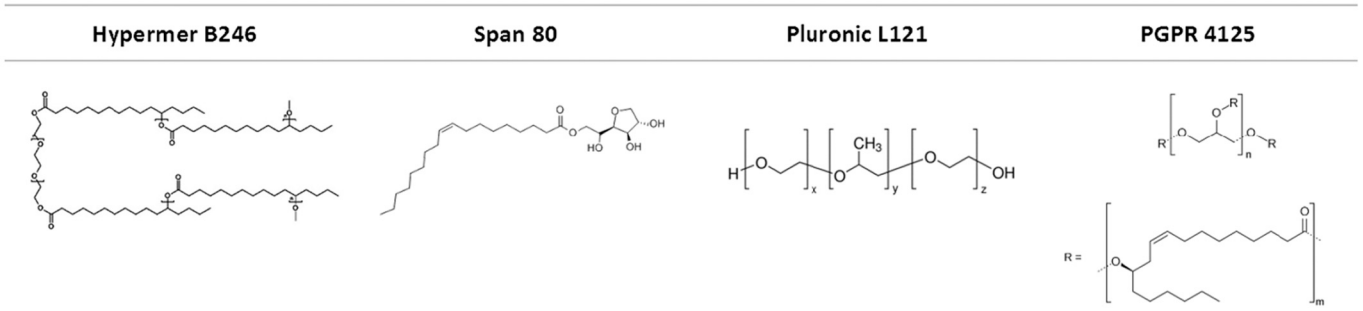

	Hypermer B246	Span 80	Pluronic L121	PGPR 4125
Structure	ABA block copolymer A: polyhydroxystearic acid as stabilizing chain B: polyethylene oxide as an anchoring group	Polyethoxylated sorbitan and oleic acid	Poly(ethylene glycol)-block-poly(propylene glycol)-block-poly(ethylene glycol)	Glycerol and fatty acids
Molecular weight (g/mol)	5000	428	~4,400	NA
HLB value	5-6	4.3	1	~3
Type	Non-ionic	Non-ionic	Non-ionic	Non-ionic
Form at RT	wax	liquid	liquid	liquid
Solubility in water	insoluble	insoluble	soluble	Glycerol: soluble Fatty acids: insoluble

Fig. 4. Surfactants used in the scope of this study and their structures and properties.

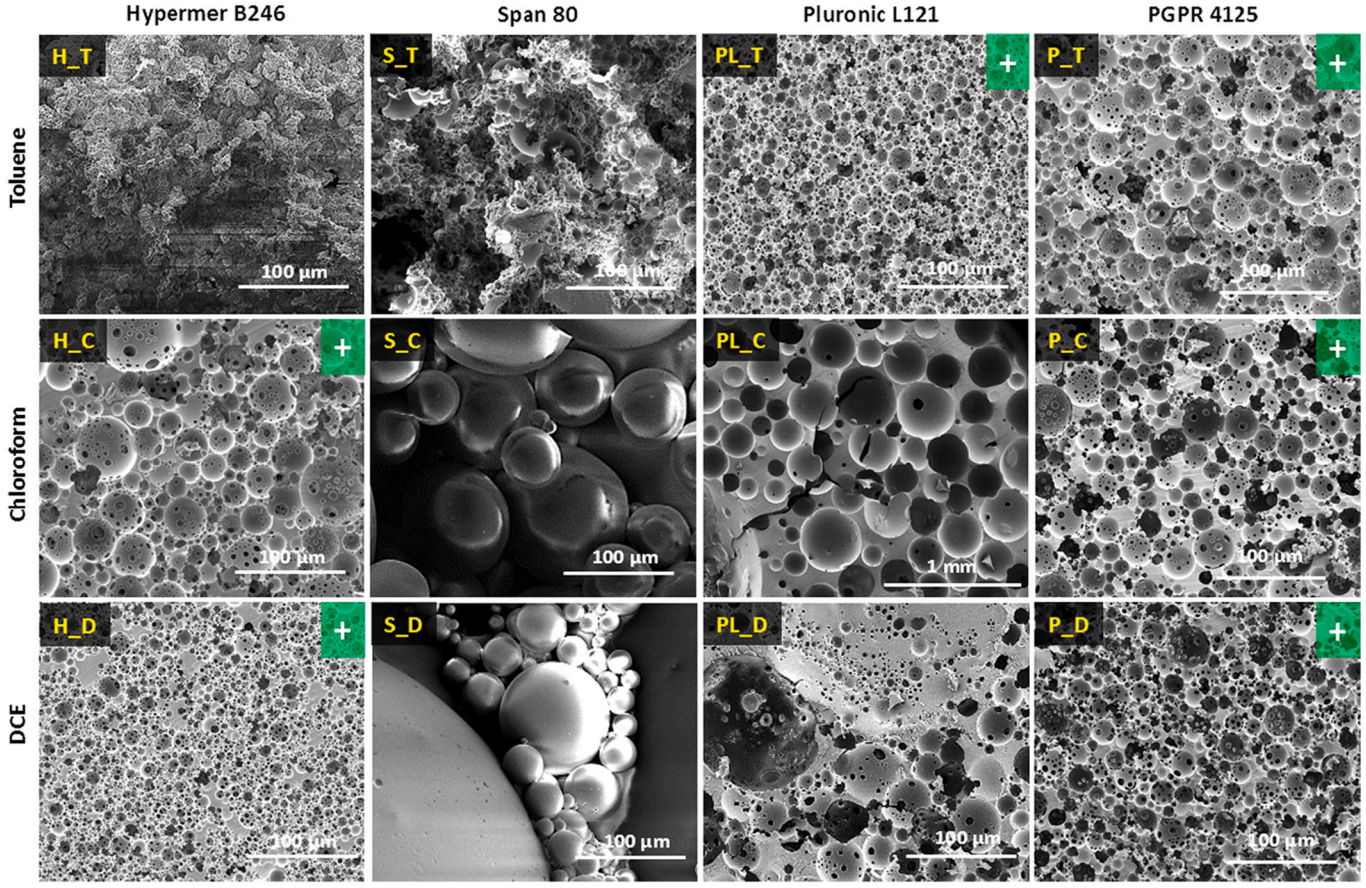

Fig. 5. SEM micrographs of 4PCLMA PolyMIPEs prepared using various surfactant and solvent systems. Solvent concentration (10% of the polymer, *w*/w), solvent volume (0.2 mL, 100% of the polymer, *v*/*w*) and internal phase volume (70%) values were constant for all groups. Samples that were (i) successful in the formation of w/o emulsion, (ii) did not show any visible phase separation and (iii) resulted in an open cellular structure are labelled with + sign in a green box. (For interpretation of the references to colour in this figure legend, the reader is referred to the web version of this article.)

Table 1
Properties of the PolyMIPEs that were prepared using various solvent and surfactant pairs. Samples that were (i) successful in the formation of w/o emulsion, (ii) did not show any visible phase separation, and (iii) resulted in an open cellular structure were labelled with *. (a) after water incorporation, the colour of the mixture turned into a white mayonnaise-like form which is a general form of an emulsion, (b) once mixing stopped, during the transfer of the MIPE to mould and curing, visible water separation from MIPE, (c) typical open cellular structure.

Sample	Surfactant type	Solvent type	$\rho_{oil\ phase}$ (g/mL)	$D_{PolyMIPE}$ (μm)	$d_{PolyMIPE}$ (μm)	$DI_{PolyMIPE}$ (d/D)	Emulsion formed[a]	Visible separation on MIPE[b]	Cellular structure[c]
H_T	Hypermer B246	Toluene	0.991	–	–	–	yes (w/o)	no	no
H_C*	Hypermer B246	Chloroform	1.283	24 ± 15	4 ± 2	0.160	yes (w/o)	no	yes
H_D*	Hypermer B246	DCE	1.171	11 ± 5	2 ± 1	0.218	yes (w/o)	no	yes
S_T	Span 80	Toluene	0.993	–	–	–	no	no	no
S_C	Span 80	Chloroform	1.286	–	–	–	yes (o/w)	yes	no
S_D	Span 80	DCE	1.174	–	–	–	yes (o/w)	yes	no
PL_T*	Pluronic L121	Toluene	0.994	10 ± 4	2 ± 1	0.196	yes (w/o)	no	yes
PL_C	Pluronic L121	Chloroform	1.287	240 ± 99	–	–	yes (w/o)	yes	yes
PL_D	Pluronic L121	DCE	1.175	142 ± 111	4 ± 3	0.091	yes (w/o)	yes	yes
P_T*	PGPR 4125	Toluene	0.991	25 ± 13	3 ± 2	0.111	yes (w/o)	no	yes
P_C*	PGPR 4125	Chloroform	1.283	22 ± 11	4 ± 2	0.160	yes (w/o)	no	yes
P_D*	PGPR 4125	DCE	1.171	19 ± 9	4 ± 2	0.186	yes (w/o)	no	yes

emulsion viscosity. Thus, we have suggested the use of a solvent blend made of chloroform and toluene in changing ratios for the tunability of the morphology of 4CPLMA PolyHIPEs [9]. According to the results of the current study, it seems that DCE and chloroform also can be a good pair to be used in the solvent blend to be able to provide tunability to PolyHIPE morphology.

Span 80 (Polysorbate 80, polyoxyethylene sorbitan monooleate, Mw: 428 g/mol) was the second surfactant tested with the same group of solvents. Span 80 is one of the most widely used surfactants for HIPE stabilisation [17,61–63]. It is a non-ionic type surfactant, liquid at RT, and insoluble in water. When the 4PCLMA emulsions were prepared with toluene as a diluting solvent and Span 80 as a surfactant (Fig. 5, S_T), a similar trend was observed with H_T. During the water addition stage, the colour of the composition turned from transparent to opaque white as a general behaviour of the emulsion formation and no separation was observed. However, both H_T and S_T only have grooves on the surface and failed to form cellular morphology. When the emulsion was prepared with chloroform or DCE as a diluting solvent and Span 80 as a surfactant (S_C and S_D), phase separation was observed even during emulsification. When the mixing was stopped, the reverse emulsion (o/w) was formed, and polymer beads were fabricated after polymerisation (Fig. 5).

Span 80 is widely used in styrene/divinylbenzene-based non-degradable PolyHIPEs where porogenic solvents are not needed [62,63]. In 2000 Cameron and Barbetta reported a research article on "the influence of porogen type on the porosity, surface area and morphology of poly(divinylbenzene) PolyHIPE foams" [6]. They used Span 80 as a surfactant and tested three different solvents; toluene, chlorobenzene, and 2-chloroethylbenzene. They reported the formation of open cellular PolyHIPEs with the use of toluene as a diluting solvent.

Christenson et al. also used toluene as a diluting solvent in Span 80 stabilised fumarate-based PolyHIPEs, and they reported the successful fabrication of porous biodegradable matrices [17]. However, there are a couple of details worth discussing here. In that study, at the same monomer composition, changing toluene concentration was seen to have an impact on the final product. While the use of 60% toluene as a diluting solvent failed to form an emulsion, the composition diluted with 40% toluene results in macroporous morphology. (i) It can be concluded that diluting solvent volume has an impact on the final morphology. One more thing to note here is that, as opposed to DVB-based PolyHIPEs mentioned in the previous paragraph, fumarate-based HIPE composition prepared with Span80 and toluene resulted in closed cellular morphology. (ii) This situation suggests the impact of monomer type on the final PolyHIPE morphology. Lastly, in both of the studies, potassium persulfate and calcium chloride are included in the aqueous phase to increase stability. So, (iii) these salts may have an impact on the emulsion stability and morphology [8]. Overall, the scenario behind the changing performance of Span 80 on different emulsion systems is very complex. However, some of the reasons are likely to be due to the type of monomer, presence/volume of diluting solvents, and presence of salts in the aqueous phase.

As a third surfactant Pluronic L121 (Mw: ~4400 g/mol), poly (ethylene glycol)-*block*-poly(propylene glycol)-*block*-poly(ethylene glycol) based non-ionic surfactant with HLB value of 1 was tested. Although all the groups prepared with Pluronic L121 successfully formed an emulsion and showed cellular structure (Fig. 5, PL_T, PL_C, and PL_D), there was a visible separation in PL_C and PL_D when the mixing stopped just before polymerisation. Successful fabrication of open porous, polyester-type of PolyHIPEs using toluene and Pluronic L121 as a diluting solvent and surfactant, respectively, have also been reported in the literature [19,64,65].

Lastly, PGPR 4125, which is a glycerol and fatty acid-based non-ionic, liquid (at RT) surfactant with an HLB value of 3, was tested. It is widely used in the chocolate industry, and it has also been reported to be included in the composition of HIPEs developed for injectable bone tissue engineering applications where the composition does not (and must not) include any toxic porogenic solvents [30,66,67]. PGPR was the only surfactant that did not create any observable phase separation in all three emulsion formulations diluted with different solvents before emulsification. All PolyMIPEs prepared with PGPR resulted in open cellular architecture (Fig. 5 P_T, P_C, and P_D).

Although all the samples presented in Fig. 5 were prepared using the constant concentration of surfactant and the same solvent volume, a significant pore and window size difference was seen between some of the groups prepared with the same surfactant but different solvents (Table 1). For example, when the composition is prepared using chloroform as a diluting solvent and Hypermer as a surfactant (H_C), the pore and window sizes are 24 ± 15 μm and 4 ± 2 μm, respectively. When DCE was used as a diluting solvent and Hypermer as a surfactant (H_D), the pore size and window sizes were 11 ± 5 μm and 2 ± 1 μm,

respectively. On the opposite of this almost two-fold size difference, emulsions prepared with PGPR as a surfactant but different diluting solvents have more similar average pore sizes.

Independent of the success of toluene in contributing to forming a cellular structure with the paired surfactants, we have not observed any visible separation in groups in which toluene is used as diluting solvent. This could be because, even if the toluene and surfactant pair fail to perform a good stabilising performance, as the density of the oil phase is close to the density of the internal phase, according to Stoke's equation, droplet movement is very slow, and no visible separation was observed.

The densities of oil phases prepared using toluene, chloroform and DCE were calculated as 0.992 ± 0.001 g/mL, 1.285 ± 0.002 g/mL, and 1.173 ± 0.002 g/mL, respectively, for all surfactant groups. As the density difference between the water and oil phase (Δρ) increases, the velocity of a single droplet in the emulsion (v) increases proportionally according to Stoke's equation (Eq. 2);

$$v = D^2 \Delta \rho g / 18n \quad (2)$$

where D is the droplet diameter under gravitational force, n is the viscosity of the oil phase, and g is the gravitational force [9].

Overall, it can be summarised that diluting solvent type has a strong impact on the efficiencies of different surfactants to stabilise the emulsions and the morphologies of PolyMIPEs and PolyHIPEs. The synergistic effect of various parameters may cause this significant difference, such as the chemical structure of solvent and surfactant, solubility, density, and polarity of the solvent, the solubility of surfactant in the

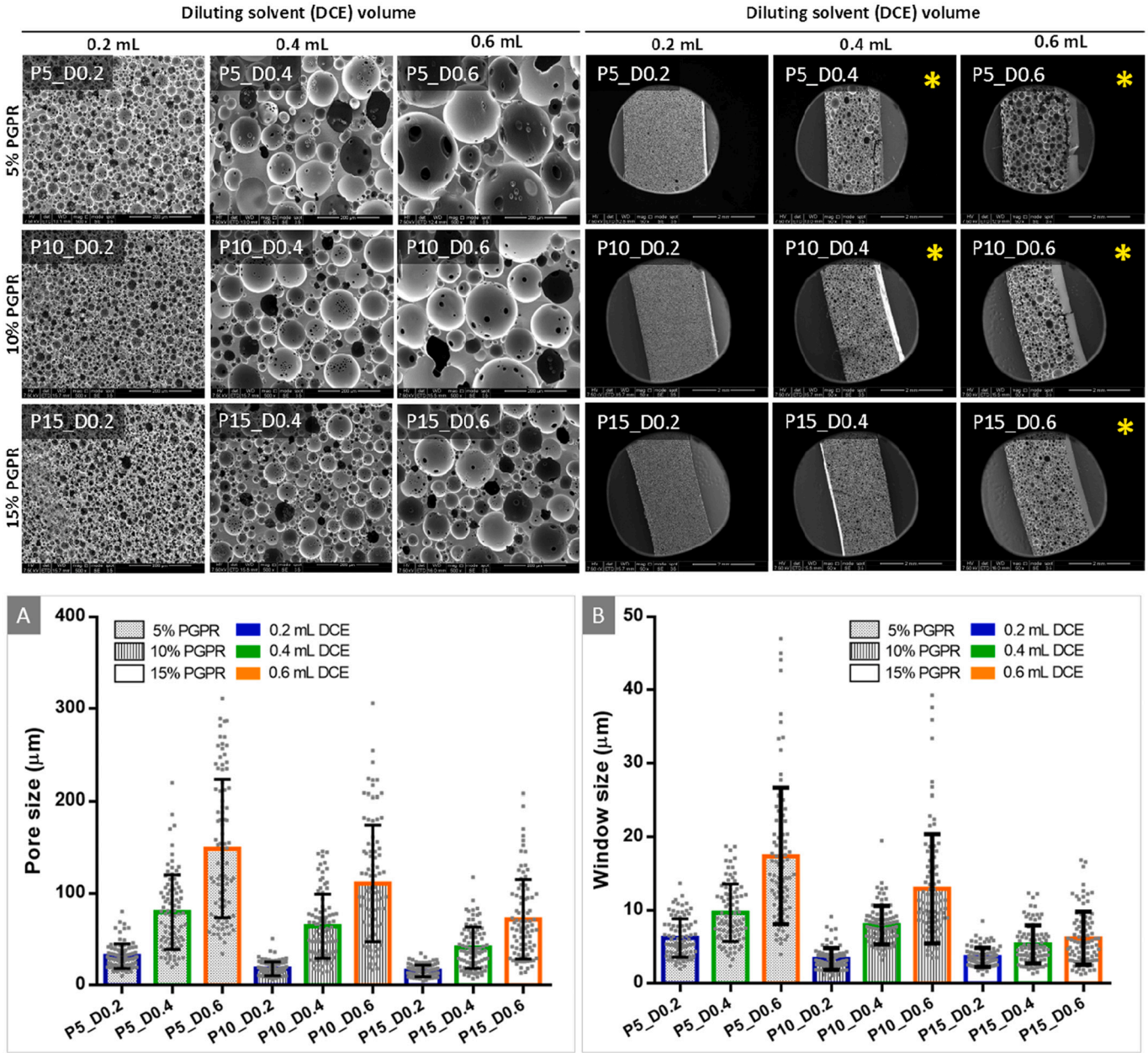

Fig. 6. SEM images showing the effect of diluting solvent volume and surfactant concentration on 4PCLMA PolyMIPE morphologies. (*) Groups that have separated a layer of polymerised nonporous oil phase on the SEM images. (A, B) Pore and window size distributions of those groups. Error bars represent the standard deviation (SD) from the average diameter.

solvent, the type of polymer, and internal phase, the solubility of the polymer in the diluting solvent. Fig. 5 gives an informative data set for the researchers to select their solvent-surfactant pair for 4PCLMA PolyMIPE development. In the light of these findings, various solvent blends can be used for the fabrication and tunability of the morphology of 4CPLMA PolyMIPE matrices. H_C, H_D, PL_T, P_T, P_C, and P_D were the groups that (i) were successful in emulsion formation, (ii) did not show any visible phase separation and (iii) resulted in an open cellular structure. For the rest of the experiments, PGPR and DCE were selected as surfactants and diluting solvents for the fabrication of 4PCLMA PolyMIPEs.

3.3. Diluting solvent volume and surfactant concentration synergistically affect the morphology of PolyMIPEs

When the emulsions were prepared using 5% PGPR (*w*/w, polymer) as a surfactant, increasing DCE volume increased the average pore sizes of the compositions drastically. Average pore sizes of the MIPEs diluted using 0.2 mL, 0.4 mL and 0.6 mL diluting solvent were found as 32 ± 13 μm, 80 ± 41 μm, and 148 ± 75 μm, respectively. While P5_D0.2 was very viscous before emulsification and needed to be transferred to the mould using a spatula, P5_D0.4 and P5_D0.6 were comparably runny and easily transferred into the mould by pouring. There was no observable separation in P5_D0.2 and P5_D0.4 but in P5_D0.6. As the large droplets are more energetically favoured, the large distribution of the droplet size is more likely to cause Ostwald ripening, which would end up with phase separation [68].

Densities and porosities of P5_D0.2, P5_D0.4, and P5_D0.6 were 0.29 g/cm^3, 0.34 g/cm^3, and 0.37 g/cm^3 and 74%, 70%, and 67%, respectively. The increasing density of the PolyMIPEs from P5_D0.2 to P5_D0.6 can be because of the separated layer of the nonporous oil phase, and this may cause a reduction in the porosity of the samples. However, there is a significant increase in the density of P15_D0.2 and P15_D0.4, although there was no separated layer in these samples. This is probably due to the increased amount of shrinkage of the samples with increasing diluting solvent volume. ~18%, 30% and 35% shrinkages were measured in all dimensions of the samples diluted with 0.2 mL, 0.4 mL and 0.6 mL, diluting solvent, respectively (in all samples prepared in this section). The correlation between dilution rate and degree of shrinkage is not linear. Bikel et al. also have shown a non-linear relationship between polymer concentration and the shrinkage of the polymer films [69]. However, in our study, this can be potentially partly due to the increasing thickness of the separated layer in a group diluted with 0.6 mL (Fig. 6, Column 6) that creates solid support, which limits the shrinkage of the whole sample. This shrinkage may also have a role in this significant difference between densities and porosities of PolyMIPEs [70].

As seen from P5_D0.2 to P5_D0.6, with increasing solvent volume, average pore size, pore size distribution span, average window size, window size distribution span, density and shrinkage of the samples increased from P10_D0.2 to P10_D0.6 and P15_D0.2 to P15_D0.6 at constant surfactant concentrations. On the contrary, porosity, degree of interconnectivity and degree of openness values were seen to reduce with increasing solvent volume and constant surfactant concentration in all samples investigated in this section.

When the diluting solvent volume was constant, increasing surfactant concentration caused a reduction in the average pore size, pore size distribution span, average window size (except one sample), and window size distribution span. The density of the samples (±0.015 g/cm^3), the porosities (±1%) and % shrinkages of these samples were very similar, showing that surfactant concentration does not affect these parameters of 4PCLMA PolyMIPEs.

The impact of changing solvent volume and surfactant concentration on some of the characteristics of MIPEs and PolyMIPEs are summarised in Fig. 7.

Increasing surfactant concentration (i) increases the emulsion stability by reducing the interfacial tension between immiscible liquids of the emulsion and (ii) reduces the average pore size of the PolyMIPEs due to the same reason [23,30,71]. On the other side, increasing diluting solvent volume (i) reduces the emulsion stability by reducing the viscosity of the oil phase according to Stoke's equation and (ii) it increases the pore size of the PolyMIPEs [9]. The reduction in the viscosity of the polymer solution and the polymer concentration are not necessarily directly correlated. In our previous study, we have shown that increasing solvent volume from 0.25 mL to 0.40 mL reduces the oil phase viscosity 2-fold; however, a further increase of the solvent volume to 0.55 mL does not result in more than a 0.25-fold reduction in the viscosity of the oil phase [9]. Similar trends were reported by other researchers with different polymers, and it has been explained with critical entanglement concentration [72–74]. After a critical polymer viscosity where polymer chain entanglements start to occur, there is a sharp increase in the polymer viscosity with increasing polymer concentration.

When working with a polymer that needs to be diluted using porogenic solvents, it is important to know that this opposite impact of increasing surfactant concentration and/or solvent volume on PolyMIPE morphology to be able to control the final morphology. In this section, we established the extent of this impact individually and synergistically to be able to control the final morphology of 4PCLMA more precisely.

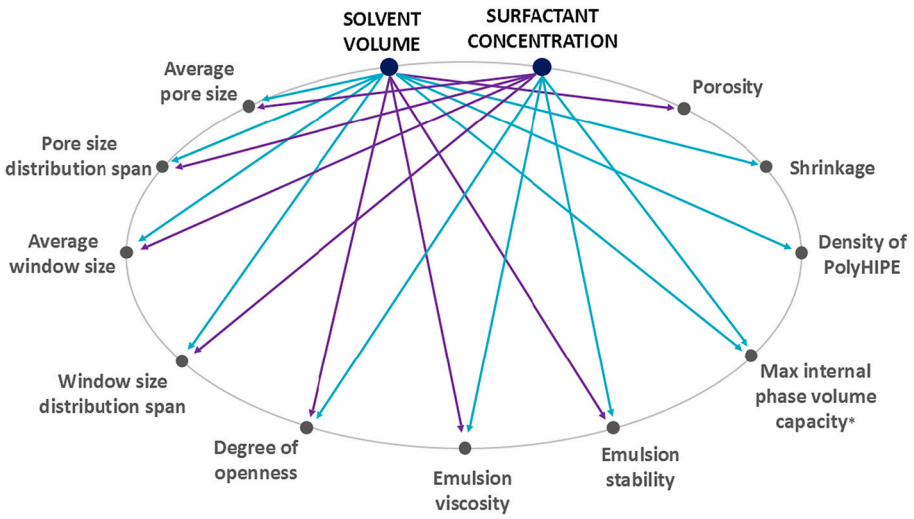

Fig. 7. Impact of changing solvent volume and surfactant concentration on characteristics of MIPEs/HIPEs and PolyMIPEs/PolyHIPEs. Blue arrows indicate one-way direct proportionality, and purple arrows indicate one-way reciprocal proportionality (*if there is enough surfactant in the system and the emulsion viscosity does not limit the incorporation of the higher volume of water). (For interpretation of the references to colour in this figure legend, the reader is referred to the web version of this article.)

3.4. Diluting solvent volume and surfactant concentration synergistically affect the maximum internal phase volume that can be incorporated into 4PCLMA HIPE composition

Following the investigation of the increasing solvent volume and surfactant concentration on average pore size, pore size distribution span, average window size, window size distribution span, density, shrinkage, porosity, degree of interconnectivity, and degree of openness in the previous section, in this section, we aimed to test their effect on maximum internal phase volume that can be incorporated into HIPE compositions without any observable phase separation (emulsion capacity).

The porosity of PolyHIPEs can be increased by increasing the internal phase volume of emulsions. The development of materials with high porosity is crucial for tissue engineering scaffolds. The high porosity is not desired for grafts developed for regeneration of load-bearing bones, as the higher porosity reduces the mechanical strength of the scaffolds. However, for soft tissues that need to be well vascularised, scaffolds with high porosity will enable endothelial cell migration and metabolic component diffusion within the scaffold [75].

When the emulsions were prepared using 5% PGPR (*w*/w, polymer) as a surfactant, increasing solvent volume did not change the maximum water volume that can be incorporated into HIPE composition, and a maximum of 3 mL of water could be added into HIPEs. However, this resulted in 88%, 83% and 78% internal phase volume for P5_D0.2′, P5_D0.4′ and P5_D0.6′, respectively. There was a significant difference between the forms of the HIPEs. While P5_D0.2′ was very viscous and needed to be transferred into a mould using a spatula, P5_D0.4′ and P5_D0.6′ were runny and could be poured into the mould easily. It can be concluded that for groups P5_D0.2′-P5_D0.6′, the limiting factor was not

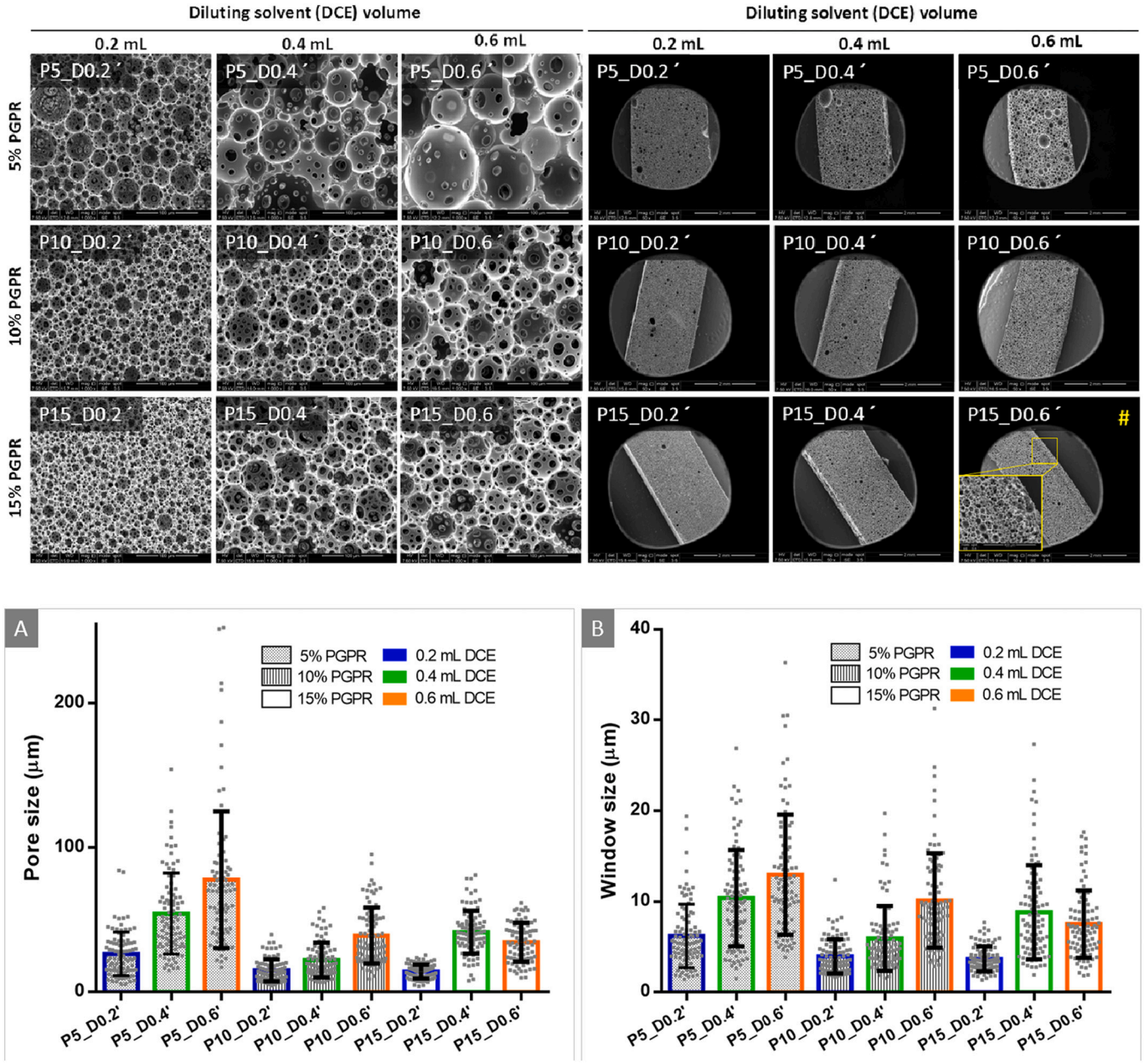

Fig. 8. SEM images showing morphologies of 4PCLMA PolyHIPEs using the changing volume of diluting solvent volume and surfactant concentration and maximum amount of internal phase volume that could be added. (#) The group that has collapsed region the SEM image. (Bottom) Pore and window size distributions of those groups. Error bars represent the standard deviation (SD) from the average diameter.

Table 2
Properties of the PolyMIPEs that were prepared using changing solvents volumes and surfactant concentrations with constant internal phase volume. (a) While the emulsion was transferred into the mould, viscous groups needed to be transferred using a spatula as they could not be poured, groups with low viscosity were easily poured into the moulds. After water incorporation, the colour of the mixture turned into a white mayonnaise-like form which is a general form of emulsions, (b) once mixing stopped, during the transfer of the MIPE to mould and curing, visible water separation from MIPE, (c) According to SEM images, any nonporous oil phase accumulation as a layer.

Sample	Surfactant* (%)	$V_{diluting\ solvent}$ (mL)	Internal phase volume (%)	Oil phase density (g/mL)	$D_{PolyMIPE}$ (μm)	$d_{PolyMIPE}$ (μm)	$DI_{PolyMIPE}$ (d/D)	$DOO_{PolyMIPE}$	$\rho_{PolyMIPE}$ (g/cm^3)	$Porosity_{PolyMIPE}$ (%)	Observations on emulsion viscosity[a]	Visible separation on MIPE[b]	Separated layer on PolyMIPE[c]
P5_D0.2	5	0.2	70	1.18	32 ± 13	6 ± 3	0.195	0.179	0.29	74	viscous	no	no
P5_D0.4	5	0.4	61	1.20	80 ± 41	10 ± 4	0.121	0.043	0.34	70	runny	no	yes
P5_D0.6	5	0.6	55	1.22	148 ± 75	17 ± 9	0.117	0.067	0.37	67	runny	yes	yes
P10_D0.2	10	0.2	70	1.17	18 ± 8	3 ± 1	0.185	0.218	0.28	75	viscous	no	no
P10_D0.4	10	0.4	61	1.20	64 ± 35	8 ± 3	0.124	0.049	0.36	68	runny	no	yes
P10_D0.6	10	0.6	54	1.21	111 ± 64	13 ± 7	0.117	0.039	0.40	65	runny	no	yes
P15_D0.2	15	0.2	69	1.17	16 ± 6	4 ± 1	0.228	0.267	0.27	76	viscous	no	no
P15_D0.4	15	0.4	61	1.19	41 ± 23	5 ± 3	0.130	0.122	0.35	69	runny	no	no
P15_D0.6	15	0.6	54	1.21	72 ± 43	6 ± 4	0.086	0.057	0.40	65	runny	no	yes

the viscosity of the emulsion but the insufficient surfactant concentration for further water incorporation.

When P5_D0.2, P5_D0.4, P5_D0.6 are compared to P5_D0.2′, P5_D0.4′, P5_D0.6′, respectively, the only changing experimental parameter was increasing internal phase volume (Table 3). When these samples are compared, it can be seen that increasing internal phase volume reduces the average pore and window sizes and PolyHIPE density, while it increases the porosity, degree of interconnectivity, and degree of openness of the matrices.

When the emulsions were prepared using 10% PGPR (*w*/w, polymer) as a surfactant, maximum water volumes that can be incorporated into HIPE composition were increased, and they were 2.70 mL, 4.85 mL, and 5.60 mL per batch that corresponding to 86%, 88%, and 87% internal phase volumes for P10_D0.2′, P10_D0.4′, and P10_D0.6′, respectively. Accordingly, porosities were measured as 88%, 90%, and 90% for the same groups. The significant difference in the maximum internal phase volumes that could be incorporated into P10_D0.2′ and P10_D0.4′ was probably because of the high viscosity of the emulsion in P10_D0.2′. Its form was highly viscous, as expected. It is because increasing surfactant concentration from 5% to 10% at 0.2 mL diluting solvent volume reduced the average pore size from 26 μm to 15 μm. Smaller water droplets in emulsion result in higher viscosity, as more of the continuous phase locates in the interfacial layers with increasing surface area and subsequently, the free volume gets smaller. Thus, only by the addition of more porogenic solvent (from P10_D0.2′ to P10_D0.4′) the maximum internal phase volume could be increased significantly. No separation was observed during emulsification in P10_D0.2′- P15_D0.6′ when the mixing was stopped before polymerisation, and also, there was no separated layer observed on the SEM images (Fig. 8).

When the emulsions were prepared using 15% PGPR (*w*/w, polymer) as a surfactant, maximum water volumes that can be incorporated into HIPE composition were 2.35 mL, 5.60 mL, and 5.40 mL per batch that corresponding to 84%, 90%, and 86% for emulsions prepared using 0.2 mL, 0.4 mL and 0.6 mL internal phase volume for samples P15_D0.2′, P15_D0.4′, and P15_D0.6′, respectively. Porosities of the same samples were 88%, 92% and 90%. The partial collapse of the P15_D0.6′ can be seen in SEM micrography (Fig. 8). Similarly, Johnson et al. previously reported that the addition of a high volume of porogenic solvent into PCL PolyHIPE composition might result in a weak PolyHIPE structure that may collapse [18].

Although phase separation was observed in some groups prepared with lower internal phase volumes in the previous section (P5_D0.2-P15_D0.6), in this section, there was no phase separation observed in none of the groups that were prepared with higher internal phase volumes (P5_D0.2′-P15_D0.6′). All other parameters were constant between these two data sets except the internal phase volumes. When the internal phase volume was increased, average pore diameters decreased in all groups. Reduction in the pore size favours emulsion stability according to Stoke's equation, and this may be one of the reasons behind increased emulsion stability. Also, the degree of interconnectivity (DI) and degree of openness (DOO) values increased when internal phase volumes were increased (from Section 3.3 to Section 3.4; Table 2 and Table 3). As the window formation is attributed to film rupture between interconnecting pores, increasing DI and DOO may indicate that walls between droplets get thinner with increasing internal phase volume, and internal phase droplets are packed tighter.

Overall, there can be two main limiting factors for the incorporation of more internal phase volume into emulsion composition; in the first scenario, as higher internal phase volume increases the emulsion viscosity, if the emulsion viscosity is already high, no more water can be incorporated. In this situation, the more diluting solvent should be included in the system to be able to reduce the viscosity and enable an increase in the internal phase volume. This is the trend that was seen in P10_D0.2′ and P10_D0.4′, or P15_D0.2′ and P15_D0.4′. In the second scenario, there is no problem with the emulsion viscosity, but there is not enough surfactant for the stabilisation of more water. Because more

Table 3
Properties of the PolyHIPEs that were prepared using changing solvent volumes and surfactant concentrations with maximum internal phase volumes that could be incorporated. (a) While the emulsion was transferred into the mould, viscous groups needed to be transferred using a spatula as they could not be poured, groups with low viscosity were easily poured into the moulds. After water incorporation, the colour of the mixture turned into a white mayonnaise-like form which is a general form of emulsions, (b) once mixing stopped, during the transfer of the HIPE to mould and curing, visible water separation from HIPE, (c) According to SEM images, any nonporous oil phase accumulation as a layer.

Sample	$V_{diluting\ solvent}$ (mL)	Surfactant* (%)	Internal phase volume (mL)	Internal phase volume (%)	$D_{PolyHIPE}$ (μm)	$d_{PolyHIPE}$ (μm)	$DI_{PolyHIPE}$ (d/D)	$DOO_{PolyHIPE}$	$\rho_{PolyHIPE}$ (g/cm^3)	$Porosity_{PolyHIPE}$ (%)	Observations on emulsion viscosity[a]	Visible separation on HIPE[b]	Separated layer on PolyHIPE[c]
P5_D0.2′	0.2	5	3.00	88	26 ± 15	6 ± 4	0.234	0.196	0.13	88	viscous	no	no
P5_D0.4′	0.4	5	3.00	83	54 ± 28	10 ± 5	0.191	0.158	0.17	85	runny	no	no
P5_D0.6′	0.6	5	3.00	78	78 ± 47	13 ± 7	0.167	0.101	0.19	83	runny	no	no
P10_D0.2′	0.2	10	2.70	86	15 ± 8	4 ± 2	0.262	0.194	0.13	88	viscous	no	no
P10_D0.4′	0.4	10	4.85	88	22 ± 12	6 ± 4	0.266	0.211	0.11	90	runny	no	no
P10_D0.6′	0.6	10	5.60	87	39 ± 19	10 ± 5	0.258	0.181	0.11	90	runny	no	no
P15_D0.2′	0.2	15	2.35	84	14 ± 5	4 ± 1	0.258	0.217	0.13	88	viscous	no	no
P15_D0.4′	0.4	15	5.60	90	41 ± 15	9 ± 5	0.213	0.266	0.09	92	runny	no	no
P15_D0.6′	0.6	15	5.40	86	34 ± 13	8 ± 4	0.218	0.189	0.11	90	runny	no	no

water means a higher intersect area between the oil and water phase which will need a higher amount of surfactant. This situation where the increased surfactant concentration enables higher internal phase volume incorporation was seen from P5_D0.4′ to P10_D0.4′ or P5_D0.6′ to P10_D0.6′. In this section, we revealed that when the diluting solvent concentration or surfactant concentration is increased, the internal phase volume capacity of HIPEs increases if there is enough surfactant in the system and the emulsion viscosity does not limit the incorporation of the higher volume of water.

4. Conclusions

Emulsion templating is a considerably easy fabrication route for the fabrication of porous matrices. However, every little change in the system causes significant changes in the final morphology. At first glance, this may seem like a disadvantage, as every process parameter should be precisely controlled for reproducibility. However, a countless number of different morphologies can be created using the same polymer by just changing different process parameters. For this, the impact of each parameter should be studied individually to be able to understand their impact on the final product. In this study, we showed that diluting solvent type used in the emulsion composition has a strong impact on the efficiency of the surfactant. Consequently, the selected solvent and surfactant pair is one of the most important determinants of the stability of the emulsion and the morphology of the PolyHIPEs. Changing solvent and surfactant amounts were shown to have an opposite impact on various parameters such as average pore size, pore size distribution span, average window size, window size distribution span, degree of openness, emulsion viscosity, and emulsion stability. Determining the framework of these changes enables to control of all these parameters more precisely using only these two parameters. Also, it was shown that by optimisation of surfactant and solvent amounts, the internal phase volume of the emulsion can be maximised. In summary, by understanding the impact of more parameters on the structure, these porous, open cellular, 4PCLMA PolyHIPE materials can be specifically tuned for specific tissue engineering applications.

Author contributions

BAD designed and performed the experiments, conducted analysis, acquisition, and interpretation of data, statistical analysis, and writing of this paper. SD contributed to data analysis and editing of the manuscript. FC contributed to the editing of the manuscript.

Data availability

The data that support the findings of this study are available from the corresponding authors, upon reasonable request.

CRediT authorship contribution statement

Betül Aldemir Dikici: Conceptualization, Formal analysis, Funding acquisition, Methodology, Project administration, Visualization, Writing – original draft, Writing – review & editing. **Serkan Dikici:** Methodology, Writing – review & editing. **Frederik Claeyssens:** Funding acquisition, Writing – review & editing.

Declaration of Competing Interest

The authors declare that they have no known competing financial interests or personal relationships that could have appeared to influence the work reported in this paper.

Data availability

Data will be made available on request.

Acknowledgements

We acknowledge the Engineering and Physical Sciences Research Council (Grant No. EP/I007695/1) and the Medical Research Council (Grant No. MR/L012669/1) for funding the equipment used in this study. The authors also acknowledge funding from the Department of Scientific Research Projects of Izmir Institute of Technology (IZTECH-BAP, 2021-IYTE-1-0110).

References

[1] Y. Zhang, Y. Shen, Y. Chen, Y. Yan, J. Pan, Q. Xiong, W. Shi, L. Yu, Hierarchically carbonaceous catalyst with Brønsted-Lewis acid sites prepared through Pickering HIPEs templating for biomass energy conversation, Chem. Eng. J. 294 (2016) 222–235, https://doi.org/10.1016/j.cej.2016.02.092.

[2] J. Yang, G. Yang, H. Liu, L. Bai, Q. Zhang, Novel porous monolithic column using poly(high internal phase emulsion) methacrylate as materials for immunoglobulin separation performance on HPLC, Chin. J. Chem. 28 (2010) 229–234, https://doi.org/10.1002/cjoc.201090058.

[3] P.W. Small, D.C. Sherrington, Design and application of a new rigid support for high efficiency continuous-flow peptide synthesis, J. Chem. Soc. Chem. Commun. (1989) 1589–1591, https://doi.org/10.1039/C39890001589.

[4] I.J. Brown, S. Sotiropoulos, Electrodeposition of Ni from a high internal phase emulsion (HIPE) template, Electrochim. Acta 46 (2001) 2711–2720, https://doi.org/10.1016/S0013-4686(01)00481-9.

[5] D. Danninger, F. Hartmann, W. Paschinger, R. Pruckner, R. Schwödiauer, S. Demchyshyn, A. Bismarck, S. Bauer, M. Kaltenbrunner, Stretchable polymerized high internal phase emulsion separators for high performance soft batteries, Adv. Energy Mater. 10 (2020), https://doi.org/10.1002/aenm.202000467.

[6] J. Ferrer, Q. Jiang, A. Menner, A. Bismarck, An approach for the scalable production of macroporous polymer beads, J. Colloid Interface Sci. 616 (2022), https://doi.org/10.1016/j.jcis.2022.02.053.

[7] C. Stubenrauch, A. Menner, A. Bismarck, W. Drenckhan, Emulsion and foam templating—promising routes to tailor-made porous polymers, Angew. Chem. Int. Ed. 57 (2018), https://doi.org/10.1002/anie.201801466.

[8] B. Aldemir Dikici, F. Claeyssens, Basic principles of emulsion templating and its use as an emerging manufacturing method of tissue engineering scaffolds, Front. Bioeng. Biotechnol. 8 (2020) 1–32, https://doi.org/10.3389/fbioe.2020.00875.

[9] B. Aldemir Dikici, C. Sherborne, G.C. Reilly, F. Claeyssens, Emulsion templated scaffolds manufactured from photocurable polycaprolactone, Polymer 175 (2019) 243–254, https://doi.org/10.1016/j.polymer.2019.05.023.

[10] R. Owen, C. Sherborne, G.C. Reilly, F. Claeyssens, T. Paterson, N.H. Green, G. C. Reilly, F. Claeyssens, Emulsion templated scaffolds with tunable mechanical properties for bone tissue engineering, J. Mech. Behav. Biomed. Mater. 54 (2016) 159–172, https://doi.org/10.1016/j.jmbbm.2015.09.019.

[11] C. Sherborne, R. Owen, G.C. Reilly, F. Claeyssens, Light-based additive manufacturing of PolyHIPEs: controlling the surface porosity for 3D cell culture applications, Mater. Des. 156 (2018) 494–503, https://doi.org/10.1016/j.matdes.2018.06.061.

[12] R. Owen, C. Sherborne, R. Evans, G.C. Reilly, F. Claeyssens, Combined porogen leaching and emulsion templating to produce bone tissue engineering scaffolds, Int. J. Bioprinting 6 (2020) 99–113, https://doi.org/10.18063/ijb.v6i2.265.

[13] C.E. Severn, A.M. Eissa, C.R. Langford, A. Parker, M. Walker, J.G.G. Dobbe, G. J. Streekstra, N.R. Cameron, A.M. Toye, Ex vivo culture of adult CD34+ stem cells using functional highly porous polymer scaffolds to establish biomimicry of the bone marrow niche, Biomaterials 225 (2019), https://doi.org/10.1016/j.biomaterials.2019.119533.

[14] B. Aldemir Dikici, S. Dikici, G.C. Reilly, S. MacNeil, F. Claeyssens, A novel bilayer polycaprolactone membrane for guided bone regeneration: combining electrospinning and emulsion templating, Materials 12 (2019) 2643, https://doi.org/10.3390/ma12162643.

[15] B. Aldemir Dikici, G.C. Reilly, F. Claeyssens, Boosting the osteogenic and angiogenic performance of multiscale porous polycaprolactone scaffolds by in vitro generated extracellular matrix decoration, ACS Appl. Mater. Interfaces 12 (2020) 12510–12524, https://doi.org/10.1021/acsami.9b23100.

[16] S. Dikici, B. Aldemir Dikici, S.I. Bhaloo, M. Balcells, E.R. Edelman, S. MacNeil, G. C. Reilly, C. Sherborne, F. Claeyssens, Assessment of the angiogenic potential of 2-deoxy-D-ribose using a novel in vitro 3D dynamic model in comparison with established in vitro assays, Front. Bioeng. Biotechnol. 7 (2020) 1–20, https://doi.org/10.3389/fbioe.2019.00451.

[17] E.M. Christenson, W. Soofi, J.L. Holm, N.R. Cameron, A.G. Mikos, Biodegradable fumarate-based polyHIPEs as tissue engineering scaffolds, Biomacromolecules 8 (2007) 3806–3814, https://doi.org/10.1021/bm7007235.

[18] D.W. Johnson, C.R. Langford, M.P. Didsbury, B. Lipp, S.A. Przyborski, N. R. Cameron, Fully biodegradable and biocompatible emulsion templated polymer scaffolds by thiol-acrylate polymerisation of polycaprolactone macromonomers, Polym. Chem. 6 (2015) 7256–7263, https://doi.org/10.1039/c5py00721f.

[19] M. Sušec, R. Liska, G. Russmüller, J. Kotek, P. Krajnc, Microcellular open porous monoliths for cell growth by thiol-ene polymerisation of low-toxicity monomers in high internal phase emulsions, Macromol. Biosci. 15 (2015) 253–261, https://doi.org/10.1002/mabi.201400219.

[20] M.A. Bokhari, G. Akay, S. Zhang, M.A. Birch, The enhancement of osteoblast growth and differentiation in vitro on a peptide hydrogel - PolyHIPE polymer hybrid material, Biomaterials 26 (2005) 5198–5208, https://doi.org/10.1016/j.biomaterials.2005.01.040.

[21] J.L. Robinson, M.A.P. McEnery, H. Pearce, M.E. Whitely, D.J. Munoz-Pinto, M. S. Hahn, H. Li, N.A. Sears, E. Cosgriff-Hernandez, Osteoinductive PolyHIPE foams as injectable bone grafts, Tissue Eng. Part A 22 (2016) 403–414, https://doi.org/10.1089/ten.tea.2015.0370.

[22] A. Richez, H. Deleuze, P. Vedrenne, R. Collier, Preparation of ultra-low-density microcellular materials, J. Appl. Polym. Sci. 96 (2005) 2053–2063, https://doi.org/10.1002/app.21668.

[23] P. Dhavalikar, J. Shenoi, K. Salhadar, M. Chwatko, G. Rodriguez-Rivera, J. Cheshire, R. Foudazi, E. Cosgriff-Hernandez, Engineering toolbox for systematic design of polyhipe architecture, Polymers 13 (2021), https://doi.org/10.3390/polym13091479.

[24] T.E. Paterson, G. Gigliobianco, C. Sherborne, N.H. Green, J.M. Dugan, S. MacNeil, G.C. Reilly, F. Claeyssens, Porous microspheres support mesenchymal progenitor cell ingrowth and stimulate angiogenesis, APL Bioeng. 2 (2018), 026103, https://doi.org/10.1063/1.5008556.

[25] B.H.L. Oh, A. Bismarck, M.B. Chan-Park, Injectable, interconnected, high-porosity macroporous biocompatible gelatin scaffolds made by surfactant-free emulsion templating, Macromol. Rapid Commun. 36 (2015) 364–372, https://doi.org/10.1002/marc.201400524.

[26] A. Malayeri, C. Sherborne, T. Paterson, S. Mittar, I.O. Asencio, P.V. Hatton, F. Claeyssens, Osteosarcoma growth on trabecular bone mimicking structures manufactured via laser direct write, Int. J. Bioprinting 2 (2016) 67–77, https://doi.org/10.18063/IJB.2016.02.005.

[27] A. Samanta, B. Nandan, R.K. Srivastava, Morphology of electrospun fibers derived from high internal phase emulsions, J. Colloid Interface Sci. 471 (2016) 29–36, https://doi.org/10.1016/j.jcis.2016.03.012.

[28] N.R. Cameron, P. Krajnc, M.S. Silverstein, Colloidal templating, Porous Polym. (2010) 119–172, https://doi.org/10.1002/9780470929445.ch4.

[29] P. Vega-Vásquez, N.S. Mosier, J. Irudayaraj, Nanoscale drug delivery systems: from medicine to agriculture, Front. Bioeng. Biotechnol. 8 (2020), https://doi.org/10.3389/fbioe.2020.00079.

[30] R.S. Moglia, J.L. Holm, N.A. Sears, C.J. Wilson, D.M. Harrison, E. Cosgriff-Hernandez, Injectable polyHIPEs as high-porosity bone grafts, Biomacromolecules 12 (2011) 3621–3628, https://doi.org/10.1021/bm2008839.

[31] Enes Durgut, Colin Sherborne, Betül Aldemir Dikici, Gwendolen C. Reilly, Frederik Claeyssens, Preparation of Interconnected Pickering Polymerized High Internal Phase Emulsions by Arrested Coalescence, Langmuir (2022), https://doi.org/10.1021/acs.langmuir.2c01243.

[32] W. Busby, N.R. Cameron, C.A.B. Jahoda, Tissue engineering matrixes by emulsion templating, Polym. Int. 51 (2002) 871–881, https://doi.org/10.1002/pi.934.

[33] W.C. Griffin, Classification of surface-active agents by "HLB", J. Soc. Cosmet. Chem. 1 (1946) 311–326. http://ci.nii.ac.jp/naid/10004943329/.

[34] W.C. Griffin, Calculation of HLB values of non-ionic surfactants, J. Soc. Cosmet. Chem. 5 (1954) 249–256.

[35] W.D. Bancroft, The theory of emulsification, V, J. Phys. Chem. 17 (1913) 501–519, https://doi.org/10.1021/j150141a002.

[36] D. Myers, Surfactant Science and Technology, Third edition, 2005, https://doi.org/10.1002/047174607X.

[37] W. Busby, N.R. Cameron, C.A.B. Jahoda, Emulsion-derived foams (PolyHIPEs) containing poly(ε-caprolactone) as matrixes for tissue engineering, Biomacromolecules 2 (2001) 154–164, https://doi.org/10.1021/bm0000889.

[38] M.A. Woodruff, D.W. Hutmacher, The return of a forgotten polymer - polycaprolactone in the 21st century, Prog. Polym. Sci. 35 (2010) 1217–1256, https://doi.org/10.1016/j.progpolymsci.2010.04.002.

[39] Y. Lumelsky, J. Zoldan, S. Levenberg, M.S. Silverstein, R.V. December, Porous polycaprolactone - polystyrene semi-interpenetrating polymer networks synthesised within high internal phase emulsions, Macromolecules 41 (2008) 1469–1474, https://doi.org/10.1021/ma7027177.

[40] Y. Lumelsky, I. Lalush-Michael, S. Levenberg, M.S. Silverstein, A degradable, porous, emulsion-templated polyacrylate, J. Polym. Sci. Part A Polym. Chem. 47 (2009) 7043–7053, https://doi.org/10.1002/pola.23744.

[41] Y. Lumelsky, M.S. Silverstein, Biodegradable porous polymers through emulsion templating, Macromolecules 42 (2009) 1627–1633, https://doi.org/10.1021/ma802461m.

[42] U. Kuhlmann, Encyclopedia of food sciences and nutrition, J. Mol. Biol. 301 (2000) 1163–1178, https://doi.org/10.1017/CBO9781107415324.004.

[43] S. Dikici, B. Aldemir Dikici, S. MacNeil, F. Claeyssens, Decellularised extracellular matrix decorated PCL PolyHIPE scaffolds for enhanced cellular activity, integration and angiogenesis, Biomater. Sci. 9 (2021) 7297–7310, https://doi.org/10.1039/D1BM01262B.

[44] N.R. Cameron, A. Barbetta, The influence of porogen type on the porosity, surface area and morphology of poly(divinylbenzene) polyHIPE foams, J. Mater. Chem. 10 (2000) 2466–2471, https://doi.org/10.1039/B003596N.

[45] B. Aldemir Dikici, A. Malayeri, C. Sherborne, S. Dikici, T. Paterson, L. Dew, P. Hatton, I. Ortega Asencio, S. Macneil, C. Langford, N.R. Cameron, F. Claeyssens, Thiolene- and polycaprolactone methacrylate-based polymerized high internal phase emulsion (PolyHIPE) scaffolds for tissue engineering, Biomacromolecules (2021), https://doi.org/10.1021/acs.biomac.1c01129.

[46] S. Dikici, N. Mangır, F. Claeyssens, M. Yar, S. Macneil, N. Mangir, F. Claeyssens, M. Yar, S. Macneil, Exploration of 2-deoxy-D-ribose and 17β-estradiol as alternatives to exogenous VEGF to promote angiogenesis in tissue-engineered constructs, Regen. Med. 14 (2019) 179–197, https://doi.org/10.2217/rme-2018-0068.

[47] S. Dikici, F. Claeyssens, S. MacNeil, Bioengineering vascular networks to study angiogenesis and vascularization of physiologically relevant tissue models in vitro, ACS Biomater. Sci. Eng. 6 (2020) 3513–3528, https://doi.org/10.1021/acsbiomaterials.0c00191.
[48] A. Barbetta, N.R. Cameron, Morphology and surface area of emulsion-derived (PolyHIPE) solid foams prepared with oil-phase soluble porogenic solvents: span 80 as surfactant, Macromolecules 37 (2004) 3188–3201, https://doi.org/10.1021/ma0359436.
[49] S. Huš, M. Kolar, P. Krajnc, Tailoring morphological features of cross-linked emulsion-templated poly(glycidyl methacrylate), Des. Monomers Polym. 18 (2015) 698–703, https://doi.org/10.1080/15685551.2015.1070503.
[50] I. Pulko, P. Krajnc, High internal phase emulsion templating - a path to hierarchically porous functional polymers, Macromol. Rapid Commun. 33 (2012) 1731–1746, https://doi.org/10.1002/marc.201200393.
[51] Q.L. Loh, C. Choong, Three-dimensional scaffolds for tissue engineering applications: role of porosity and pore size, Tissue Eng. Part B Rev. 19 (2013) 485–502, https://doi.org/10.1089/ten.teb.2012.0437.
[52] I. Barbara, M.-A. Dourges, H. Deleuze, Preparation of porous polyurethanes by emulsion-templated step growth polymerisation, Polymer 132 (2017) 243–251, https://doi.org/10.1016/j.polymer.2017.11.018.
[53] M. Ovadia, M.S. Silverstein, High porosity, responsive hydrogel copolymers from emulsion templating, Polym. Int. 65 (2016) 280–289, https://doi.org/10.1002/pi.5052.
[54] X. Wan, U. Azhar, Y. Wang, J. Chen, A. Xu, S. Zhang, B. Geng, Highly porous and chemical resistive P(TFEMA-DVB) monolith with tunable morphology for rapid oil/water separation, RSC Adv. 8 (2018), https://doi.org/10.1039/c8ra00501j.
[55] Y. Wang, U. Azhar, J. He, H. Chen, J. Zhao, A.M. Pang, B. Geng, A facile fabrication of porous fluoro-polymer with excellent mechanical properties based on high internal phase emulsion templating using PLA as co-stabiliser, RSC Adv. 9 (2019), https://doi.org/10.1039/c9ra08226c.
[56] J. Feng, Q. Chen, X. Wu, S.M. Jafari, D.J. McClements, Formulation of oil-in-water emulsions for pesticide applications: impact of surfactant type and concentration on physical stability, Environ. Sci. Pollut. Res. 25 (2018), https://doi.org/10.1007/s11356-018-2183-z.
[57] M. Zhou, R. Foudazi, Effect of cosurfactant on structure and properties of polymerized high internal phase emulsions (PolyHIPEs), Langmuir 37 (2021), https://doi.org/10.1021/acs.langmuir.1c00419.
[58] M.I. Azman, N. Kwangsawart, J. Preechawong, M. Nithitanakul, P. Sapsrithong, Fabrication of poly(Pentaerythritol tetrakis (3-mercaptopropionate)/dipentaerythritol penta−/hexa-acrylate)hipes macroporous scaffold with alpha hydroxyapatite via photopolymerisation for fibroblast regeneration, Crystals 10 (2020), https://doi.org/10.3390/cryst10090746.
[59] S.A. Richardson, T.M. Rawlings, J. Muter, M. Walker, J.J. Brosens, N.R. Cameron, A.M. Eissa, Covalent attachment of fibronectin onto emulsion-templated porous polymer scaffolds enhances human endometrial stromal cell adhesion, infiltration, and function, Macromol. Biosci. 19 (2019) 1–10, https://doi.org/10.1002/mabi.201800351.
[60] S. Caldwell, D.W. Johnson, M.P. Didsbury, B.A. Murray, J.J. Wu, S.A. Przyborski, N.R. Cameron, Degradable emulsion-templated scaffolds for tissue engineering from thiol-ene photopolymerisation, Soft Matter 8 (2012) 10344–10351, https://doi.org/10.1039/c2sm26250a.
[61] S.J. Pierre, J.C. Thies, A. Dureault, N.R. Cameron, J.C.M. Van Hest, N. Carette, T. Michon, R. Weberskirch, Covalent enzyme immobilisation onto photopolymerised highly porous monoliths, Adv. Mater. 18 (2006) 1822–1826, https://doi.org/10.1002/adma.200600293.
[62] G. Akay, M.A. Birch, M.A. Bokhari, Microcellular polyHIPE polymer supports osteoblast growth and bone formation in vitro, Biomaterials 25 (2004) 3991–4000, https://doi.org/10.1016/j.biomaterials.2003.10.086.
[63] M.W. Hayman, K.H. Smith, N.R. Cameron, S.A. Przyborski, Growth of human stem cell-derived neurons on solid three-dimensional polymers, J. Biochem. Biophys. Methods 62 (2005) 231–240, https://doi.org/10.1016/j.jbbm.2004.12.001.
[64] M. Paljevac, L. Gradišnik, S. Lipovšek, U. Maver, J. Kotek, P. Krajnc, Multiple-level porous polymer monoliths with interconnected cellular topology prepared by combining hard sphere and emulsion templating for use in bone tissue engineering, Macromol. Biosci. 18 (2018), https://doi.org/10.1002/mabi.201700306.
[65] J. Naranda, M. Sušec, U. Maver, L. Gradišnik, M. Gorenjak, A. Vukasović, A. Ivković, M.S. Rupnik, M. Vogrin, P. Krajnc, Polyester type polyHIPE scaffolds with an interconnected porous structure for cartilage regeneration, Sci. Rep. 6 (2016) 28695, https://doi.org/10.1038/srep28695.
[66] J.L. Robinson, R.S. Moglia, M.C. Stuebben, M.A.P. Mcenery, E. Cosgriff-Hernandez, Achieving interconnected pore architecture in injectable PolyHIPEs for bone tissue engineering, Tissue Eng. Part A 20 (2014) 1103–1112, https://doi.org/10.1089/ten.tea.2013.0319.
[67] R.S. Moglia, M. Whitely, P. Dhavalikar, J. Robinson, H. Pearce, M. Brooks, M. Stuebben, N. Cordner, E. Cosgriff-Hernandez, Injectable polymerised high internal phase emulsions with rapid in situ curing, Biomacromolecules 15 (2014) 2870–2878, https://doi.org/10.1021/bm500754r.
[68] V. Zanatta, K. Rezzadori, F.M. Penha, G. Zin, E. Lemos-Senna, J.C.C. Petrus, M. Di Luccio, Stability of oil-in-water emulsions produced by membrane emulsification with microporous ceramic membranes, J. Food Eng. 195 (2017) 73–84, https://doi.org/10.1016/j.jfoodeng.2016.09.025.
[69] M. Bikel, I.G.M. Pünt, R.G.H. Lammertink, M. Wessling, Shrinkage effects during polymer phase separation on microfabricated molds, J. Membr. Sci. 347 (2010), https://doi.org/10.1016/j.memsci.2009.10.015.
[70] J.-H. Chen, T. Le, K.-C. Hsu, Application of PolyHIPE membrane with tricaprylmethylammonium chloride for Cr(VI) ion separation: parameters and mechanism of transport relating to the pore structure, Membranes 8 (2018) 11, https://doi.org/10.3390/membranes8010011.
[71] J.M. Williams, A.J. Gray, M.H. Wilkerson, Emulsion stability and rigid foams from styrene or divinylbenzene water-in-oil emulsions, Langmuir 6 (1990), https://doi.org/10.1021/la00092a026.
[72] E. Zhang, X. Dai, Z. Dong, X. Qiu, X. Ji, Critical concentration and scaling exponents of one soluble polyimide - from dilute to semidilute entangled solutions, Polymer 84 (2016), https://doi.org/10.1016/j.polymer.2016.01.001.
[73] D. Han, A.J. Steckl, Coaxial electrospinning formation of complex polymer fibers and their applications, Chempluschem. 84 (2019), https://doi.org/10.1002/cplu.201900281.
[74] A.V. Dobrynin, Solutions of charged polymers, in: Polym. Sci. A Compr. Ref. 10 Vol. Set, 2012, https://doi.org/10.1016/B978-0-444-53349-4.00005-4.
[75] P. Yadav, G. Beniwal, K.K. Saxena, A review on pore and porosity in tissue engineering, Mater. Today Proc. 44 (2021) 2623–2628, https://doi.org/10.1016/j.matpr.2020.12.661.